


RESEARCH ARTICLE

Near-infrared light scattering and water diffusion in newborn brains

Sachiko Iwata^{1,2}, Reiji Katayama³, Kennosuke Tsuda^{1,2}, Yung-Chieh Lin⁴, Tsuyoshi Kurata², Masahiro Kinoshita², Koya Kawase¹, Takenori Kato¹, Shin Kato¹, Tadashi Hisano¹, Motoki Oda⁵, Etsuko Ohmae⁵, Sachio Takashima⁶, Yuko Araki⁷, Shinji Saitoh¹ & Osuke Iwata^{1,2} 

¹Center for Human Development and Family Science, Department of Pediatrics and Neonatology, Nagoya City University Graduate School of Medical Sciences, Nagoya, Aichi, 467-8601, Japan

²Department of Paediatrics and Child Health, Centre for Developmental and Cognitive Neuroscience, Kurume University School of Medicine, Kurume, Fukuoka, 830-0011, Japan

³Centre for the Study of Medical Education, Kurume University School of Medicine, Kurume, Fukuoka, 830-0011, Japan

⁴Department of Pediatrics, National Cheng Kung University Hospital, College of Medicine, National Cheng-Kung University, Tainan, 70457, Taiwan

⁵Central Research Laboratory, Hamamatsu Photonics K.K., Hamamatsu, Shizuoka, 434-8601, Japan

⁶Yanagawa Institute for Developmental Disabilities, International University of Health and Welfare, Yanagawa, Fukuoka, 832-0813, Japan

⁷Graduate School of Information Sciences, Tohoku University, Sendai City, Miyagi, 980-8579, Japan

Correspondence

Osuke Iwata, Department of Pediatrics and Neonatology, Nagoya City University Graduate School of Medical Sciences, 1 Kawasumi, Mizuho, Nagoya, Aichi 467-8601, Japan. Tel: (+81) 52 853 8246; Fax: (+81) 52 842 3449; E-mail: o.iwata@med.nagoya-u.ac.jp

Funding Information This study was funded by the Japanese Ministry of Education, Culture, Sports, Science and Technology (Grant-in-Aid for Scientific Research, 20H00102) and the Japan Science and Technology Agency (FOREST Program, JPMJFR200I).

Received: 4 July 2022; Accepted: 19 July 2022

Annals of Clinical and Translational Neurology 2022; 9(9): 1417–1427

doi: 10.1002/acn3.51641

Abstract

Objective: MRI provides useful information regarding brain maturation and injury in newborn infants. However, MRI studies are generally restricted during acute phase, resulting in uncertainty around upstream clinical events responsible for subtle cerebral injuries. Time-resolved near-infrared spectroscopy non-invasively provides the reduced scattering coefficient (μ'_s), which theoretically reflects tissue structural complexity. This study aimed to test whether μ'_s values of the newborn head reflected MRI findings. **Methods:** Between June 2009 and January 2015, 77 hospitalised newborn infants (31.7 ± 3.8 weeks gestation) were assessed at 38.8 ± 1.3 weeks post-conceptual age. Associations of μ'_s values with MRI scores, mean diffusivity and fractional anisotropy were assessed. **Results:** Univariable analysis showed that μ'_s values were associated with gestational week ($p = 0.035$; regression coefficient [B], 0.065; 95% confidence interval [CI], 0.005–0.125), fractional anisotropy in the cortical grey matter ($p = 0.020$; B , -5.994 ; 95%CI, -11.032 to -0.957), average diffusivity in the cortical grey matter ($p < 0.001$; B , -4.728 ; 95%CI, -7.063 to -2.394) and subcortical white matter ($p = 0.001$; B , -2.071 ; 95%CI, -3.311 to -0.832), subarachnoid space ($p < 0.001$; B , -0.289 ; 95%CI, -0.376 to -0.201) and absence of brain abnormality ($p = 0.042$; B , -0.422 ; 95%CI, -0.829 to -0.015). The multivariable model to explain μ'_s values comprised average diffusivity in the subcortical white matter ($p < 0.001$; B , -2.066 ; 95%CI, -3.200 to -0.932), subarachnoid space ($p < 0.001$; B , -0.314 ; 95%CI, -0.412 to -0.216) and absence of brain abnormality ($p = 0.021$; B , -0.400 ; 95%CI, -0.739 to -0.061). **Interpretation:** Light scattering was associated with brain structure indicated by MRI-assessed brain abnormality and diffusion-tensor-imaging-assessed water diffusivity. When serially assessed in a larger population, μ'_s values might help identify covert clinical events responsible for subtle cerebral injury.

Introduction

Despite the recent decrease in mortality and morbidity rates of preterm infants, they remain at an increased risk of developing cognitive impairments, school failure and behavioural problems.¹ Qualitative assessment findings observed on brain MRI obtained at term-equivalent age are now established markers for predicting the neurological outcomes of preterm infants.^{2,3} More recent studies have also used diffusion tensor imaging (DTI) to assess brain microstructural changes based on the diffusion properties of water in the cerebral tissue.^{4–6} Furthermore, magnetic resonance spectroscopy has been utilised in clinical studies as a probe to monitor the biochemical composition and metabolic status of the cerebral tissue.^{7,8} Although these techniques have established their indispensable roles in the neurological assessment of newborn infants, at most centres, MRI studies are performed only after weaning from intensive care and shortly before discharge due to their safety, cost and technical limitations. Consequently, the role of upstream clinical events, such as subclinical hypoxia–ischaemia, malnutrition, infection and sedation, to abnormal MRI findings at the term equivalent age, remain largely unknown.

Near-infrared spectroscopy (NIRS) is a non-invasive tool that could be applied serially at the cot-side.^{9,10} Conventional continuous-wave NIRS provides information regarding the fraction of oxygenated and deoxygenated haemoglobin from the absorption coefficient (μ_a) of near-infrared light at different wavelengths.¹¹ This technique has been used to monitor cerebral oxygenation and perfusion in a wide range of subjects.^{10,12} Time-resolved NIRS (TR-NIRS) is a relatively new technique that provides additional information regarding the optical path length and scattering property of the near-infrared light.¹³ Theoretically, light scattering depends on the structural complexity of the tissue through which it passes.^{14,15} Indeed, studies in animal models have demonstrated a notable decrease in the reduced scattering coefficient (μ'_s) of the near-infrared light obtained from the head in association with hypoxic-ischaemic events and subsequent cell death.^{16–18} In clinical settings, lower μ'_s values obtained from the head were reported in association with both physiological variables and pathological events, such as younger gestational age at birth, poor nutritional status after birth and the presence of cerebral infarction.^{19–22} If microstructural information for the brain tissue could be obtained at the cot-side using TR-NIRS, covert clinical events responsible for abnormalities at term observed by MRI and higher cognitive impairments at school age might be identified early.

Therefore, this study aimed to test whether μ'_s values obtained from the head of preterm and term newborn

infants reflected the brain MRI-based macroscopic structure and DTI-assessed tissue water diffusion.

Methods

This prospective observational study was conducted in compliance with the Declaration of Helsinki and was approved by the ethics committee of the Kurume University School of Medicine (reference number: 12128 and 14218). Informed parental consent was obtained for all participating infants. Relationships between the μ'_s values and clinical variables in a portion of the current study cohort have been reported previously.^{20,21}

Study population

Newborn infants admitted to a tertiary neonatal intensive care centre (Kurume University Hospital, Kurume, Fukuoka, Japan) between June 2009 and January 2015 and whose MRI studies were scheduled before discharge as a part of a follow-up protocol for infants at high risk of brain injury, were considered as candidates for the study (Fig. 1). In this centre, infants with preterm birth <34 weeks gestation, clinical events suggestive of antenatal hypoxia–ischaemia and congenital brain anomalies are enrolled into this follow-up protocol to provide longitudinal monitoring of brain growth, maturation, injury and neurodevelopmental outcomes. For the current study, infants with chromosomal aberrations, malformation syndrome, grade III/IV intraventricular haemorrhage, congenital hydrocephalus and other major cerebral anomalies were excluded. In addition, infants who met the indication of therapeutic hypothermia were not recruited because of technical difficulties in simultaneously applying the TR-NIRS probe and electrodes for electroencephalogram. To test a multivariable model with up to three independent variables, a sample of 77 infants was required to achieve a study power of 0.8 at an alpha level of 0.05 and a beta level of 0.20 with an effect size of 0.15. Therefore, we aimed to recruit at least 85 infants in anticipation of incomplete data in up to 10% of the participants.

TR-NIRS measurement

Data were acquired when infants were asleep or calmly awake using a TR-NIRS system (TRS-10, Hamamatsu Photonics K.K., Hamamatsu, Shizuoka, Japan), as previously described.²⁰ In brief, the TR-NIRS probes were inserted within a rubber holder and applied to a flat part of the head with an inter-optode distance of 3 cm. A time-correlated single-photon counting method was used to obtain the μ'_s values for three wavelengths of 761, 791

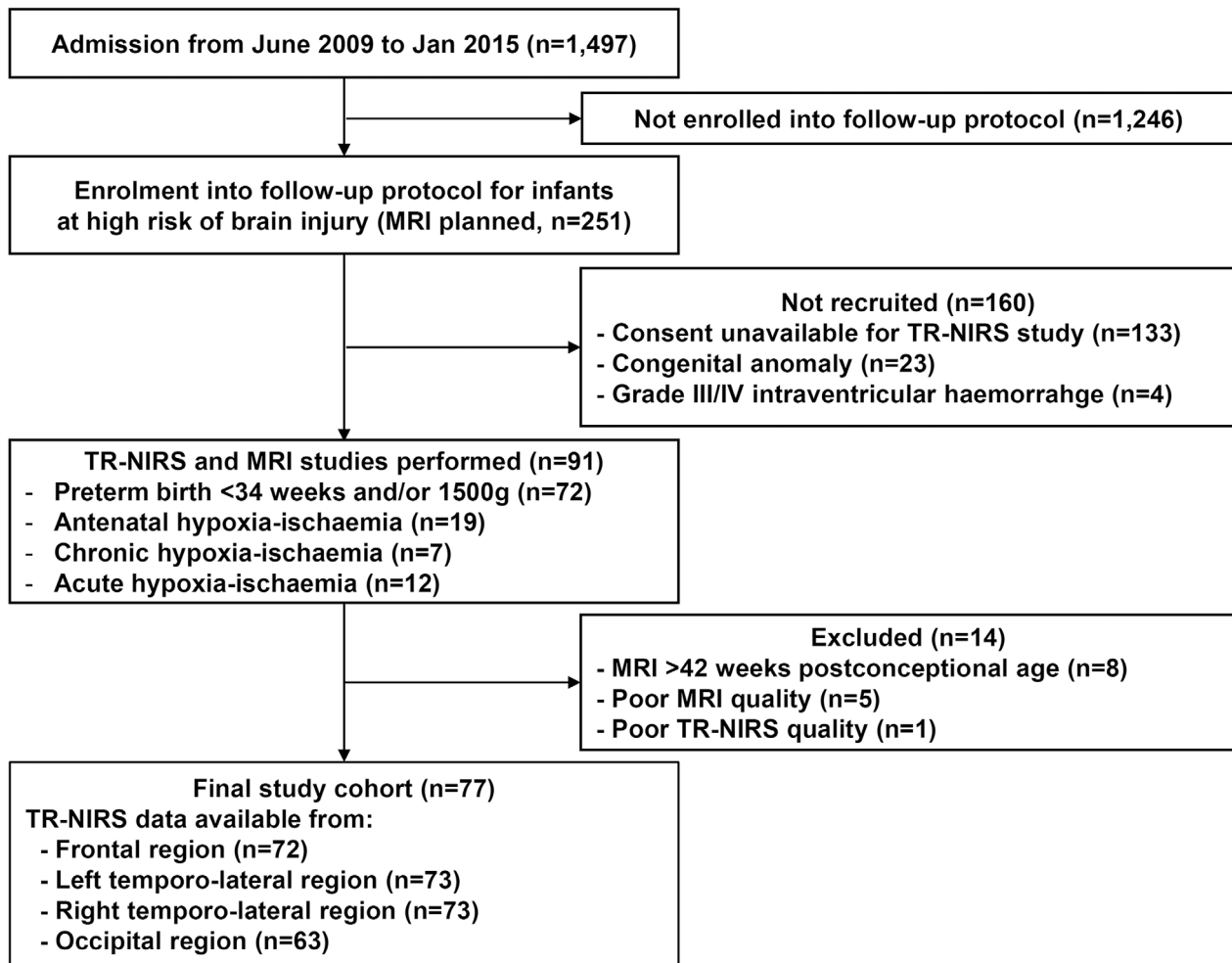


Figure 1. Study population. Flow diagram depicting the selection of participating newborn infants in the current study. MRI, magnetic-resonance imaging; TR-NIRS, time-resolved near-infrared spectroscopy.

and 836 nm in the frontal, left and right temporoparietal and occipital regions. Data collection was not performed for head regions with poor probe contact, poor fit to the photon diffusion equation or low signal-to-noise ratios with the count rate with relative dark- to peak-count ratios of >0.1 . Ten-second data acquisition was repeated five times for each head region by repositioning the probe each time; five μ'_s readings were averaged for each head region. Although data were acquired longitudinally from birth to discharge with intervals of approximately 1 week, for the current study, only TR-NIRS studies obtained closest to the MRI studies were used for comparisons with MRI findings.

MRI acquisition and assessment

A 3-Tesla Signa HDxt scanner (GE Medical Systems, Milwaukee, WI, USA) was used to acquire T1-weighted

images (repetition time [TR], 11 msec; echo time [TE], 5 msec; slice thickness, 1 mm; matrix, 384×224 ; interpolated, 512×512 ; field of view [FOV], 200×200 mm; both coronal and sagittal sections were reconstructed from axial slices), T2-weighted images (TR, 5000 msec; TE, 87 msec; slice thickness, 4 mm; matrix, 384×224 ; reconstruction matrix, 512×512 ; FOV, 200×200 mm) and a single-shot, spin-echo, planar imaging DTI sequence with isotropic resolution (TR, 15,000 msec; TE, 86 msec; slice thickness, 3 mm; matrix, 256×256 ; FOV, 240×240 mm; six directions; b values, 0 and 1000 s/mm^2). MRI and DTI data were then assessed by an experienced examiner (S.I.). Each MRI scan was visually inspected for its quality and assessed using an established MRI scoring system for brain maturation, growth and injury in the cerebral white matter (6 items), cortical grey matter (3 items), deep grey matter (2 items) and cerebellum (2 items) to give a composite score of 0–40.^{3,23}

A composite score of >4 was regarded as either mild (total score 4–7), moderate (8–11) or severe (≥ 12) brain abnormality. DTI data were analysed to determine the average diffusivity (D_{av}) and fractional anisotropy (FA) for six regions of interest (ROIs) within the right and left frontal, parietal and occipital cortices, and six adjacent white matter ROIs, using a slice dissecting the centrum semiovale (Fig. 2). These ROIs were manually placed on the T2-weighted ($b = 0 \text{ s/mm}^2$) images using an open-source JAVA-based image processing program (ImageJ, U.S. National Institutes of Health, Bethesda, MD, USA).²⁴ Since both intra- and extracerebral structures might affect the scattering property of near-infrared light, the sub-arachnoid space or the shortest distance between the top of the gyrus and the dural side of the skull was quantified on the T2-weighted image corresponding to each ROI.

Data analysis

Considering postnatal temporal changes in MRI and DTI findings over weeks,^{23,25,26} infants with TR-NIRS and MRI data obtained more than 6 days apart were not considered. Since the scattering property of near-infrared light is similar between the wavelengths used,²⁰ the mean μ'_s value at 760 nm for each brain region was used as the representative datapoint. For convenience, the DTI ROIs of the bilateral frontal and occipital regions were averaged and binned to compare with TR-NIRS data from the frontal, right parietal, left parietal and occipital regions.

All statistical analyses were conducted using the IBM SPSS Statistics for Windows, Version 25.0 (IBM Corp.,

Armonk, NY, USA) software. Unless otherwise stated, values are shown as means \pm standard deviations. Since missing data were limited to TR-NIRS measures from different head regions, multiple imputations for missing data were not performed. Before assessing the relationship between TR-NIRS and MRI/DTI data, inter-regional variations in μ'_s , D_{av} and FA were examined using repeated measure ANOVA. Statistical findings were corrected for multiple comparisons by Bonferroni correction for the four head regions.

Crude associations between the MRI/DTI findings and clinical variables and the μ'_s values were assessed using the generalised estimating equation with linear regression adjusted for the four head regions; statistical findings from the univariable analysis were not corrected for multiple comparisons because these were not part of our main objectives.²⁷ Based on our hypothesis, dependence of μ'_s on the presence of cerebral abnormality detected by conventional MRI, subarachnoid space and D_{av} values of the subcortical white matter were assessed in a multivariable model, while controlling for covariates of the head regions and gestational age at birth. Alternative models, which replaced D_{av} of the subcortical white matter with D_{av} of the cortical grey matter and FA in the cortical grey matter and subcortical white matter, were also developed to allow comparison with the first model.

Data availability

The raw data used in the current analysis are available from the corresponding author upon reasonable request.

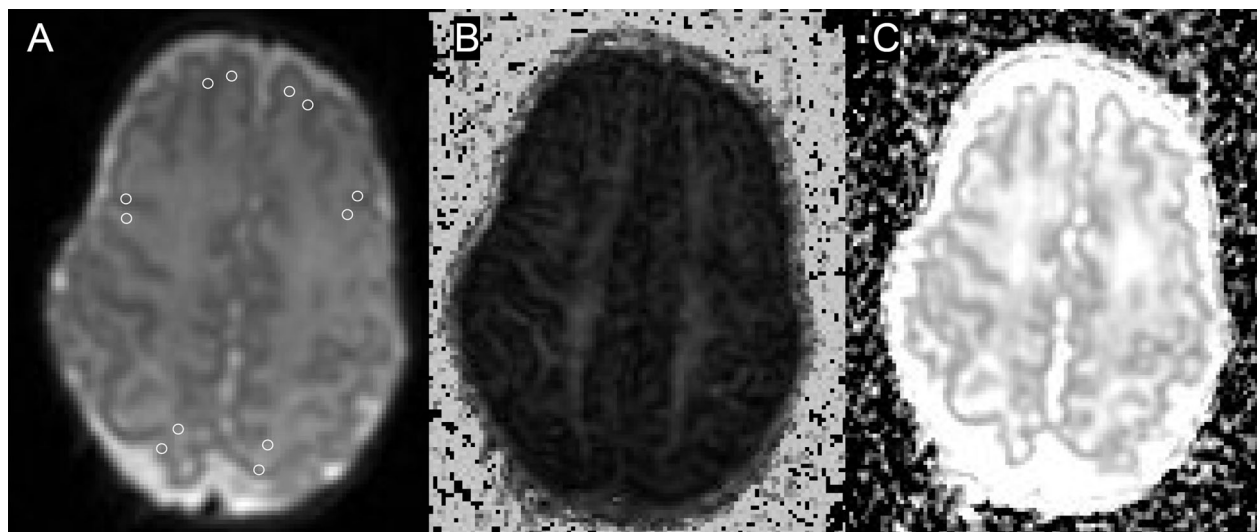


Figure 2. Placement of regions of interest in representative diffusion-tensor images. Regions of interests in the cortical grey matter and adjacent subcortical white matter (open elliptic) in T2-weighted image (A), fractional anisotropy map (B) and average diffusivity map (C) on the centrum semiovale level.

Results

During the study period, 1,497 infants were admitted to the unit, 251 of whom were enrolled into the follow-up protocol for infants at high risk of brain injury (Fig. 1). Of these, informed consent was unavailable in 133 infants, major congenital anomalies were noted in 23 infants and grade III/IV intraventricular haemorrhage was confirmed in four infants, leaving 91 infants available for the study. Indications of admission were preterm birth ($n = 72$), acute hypoxia–ischaemia ($n = 12$) and chronic hypoxia–ischaemia ($n = 7$). All the infants successfully performed TR-NIRS and MRI studies. However, head MRI was performed at postconceptional age of over 42 weeks in eight infants. MRI quality was poor because of motion artefacts in five infants. In one infant, who had developed an extensive subarachnoid and subdural haemorrhage, the TR-NIRS acquisition was not performed because of excessively weak light penetration. Data from these 14 infants were not considered further. The final cohort comprised 77 newborn infants at a gestational age of 31.7 ± 3.8 weeks, body weight of 1474 ± 550 g at birth and at postconceptional age of 38.8 ± 1.3 weeks at the time of the MRI study and 38.8 ± 1.4 weeks at the time of the TR-NIRS study (Table 1). TR-NIRS data were not collected from the frontal ($n = 5$), left temporoparietal ($n = 4$), right temporoparietal ($n = 4$) and occipital ($n = 14$) regions because of poor probe contact or insufficient light penetration. No other data were missing.

Conventional MRI findings

Cerebral abnormality with total MRI composite scores of ≥ 4 was noted in 26 infants (mild abnormality, $n = 24$; moderate, $n = 2$; severe, $n = 0$). The subarachnoid space was 3.3 ± 1.7 mm, 2.7 ± 1.1 mm, 2.3 ± 1.0 mm and 4.4 ± 2.0 mm for the frontal, left temporoparietal, right temporoparietal and occipital regions, respectively.

μ'_s values and their regional variations

The mean μ'_s value in the right temporoparietal region ($7.33 \pm 1.16/\text{cm}$) was larger than the occipital ($6.95 \pm 1.40/\text{cm}$, $p = 0.019$), left temporoparietal ($6.59 \pm 1.22/\text{cm}$, $p < 0.001$) and frontal ($5.98 \pm 1.23/\text{cm}$, $p < 0.001$) regions (See Table 2 for other inter-region comparisons).

D_{av} values and their regional variations

D_{av} values in the frontal region of the cortical grey matter ($0.985 \pm 0.064 \times 10^{-3} \text{ mm}^2/\text{s}$) were greater than in the occipital ($0.937 \pm 0.054 \times 10^{-3} \text{ mm}^2/\text{s}$, $p < 0.001$), right

Table 1. Clinical background variables of the study population.

Variables	Values
Variables at birth	
Male sex	39 (50.6)
Gestational age (week)	31.7 ± 3.8
<28 weeks	10 (13.0)
28–31 weeks	30 (39.0)
≥ 32 weeks	37 (48.1)
Body weight at birth (g)	1474 ± 550
Head circumference at birth (cm)	28.2 ± 3.2
Intrauterine growth restriction	30 (38.9)
Symmetrical	9 (11.7)
Antenatal glucocorticoid	34 (44.2)
Caesarean section	58 (75.3)
Emergency caesarean section	52 (67.5)
Multiple pregnancy	14 (18.1)
Postnatal variables	
Indomethacin for ductus arteriosus	24 (31.2)
Chronic lung disease	18 (23.4)
Postnatal glucocorticoid	18 (23.4)
Enteral feeding >100 mL/kg/day (age in day)	8 ± 5
Necrotising enterocolitis	0 (0.0)
Intestinal perforation	0 (0.0)
Recovery to the birth weight (age in day)	9 ± 5
Days on mechanical ventilation	9 ± 12
MRI brain abnormality classification	
Normal	51
Mild abnormality	24
Moderate abnormality	2
Severe abnormality	0
Postnatal age at the time of TR-NIRS study (day)	50.2 ± 26.6
Postconceptional age at the time of TR-NIRS study (week)	38.8 ± 1.4
Postnatal age at the time of MRI study (day)	49.7 ± 26.5
Postconceptional age at the time of MRI study (week)	38.8 ± 1.3

Values are shown as mean \pm standard deviation or number (%). TR-NIRS, time-resolved near-infrared spectroscopy; MRI, magnetic-resonance imaging.

temporoparietal ($0.929 \pm 0.052 \times 10^{-3} \text{ mm}^2/\text{s}$, $p < 0.001$) and left temporoparietal ($0.919 \pm 0.041 \times 10^{-3} \text{ mm}^2/\text{s}$, $p < 0.001$) regions (See Table 2 for other inter-region comparisons).

The subcortical white matter D_{av} values of the frontal region ($1.330 \pm 0.126 \times 10^{-3} \text{ mm}^2/\text{s}$) were similar to the occipital region ($1.319 \pm 0.165 \times 10^{-3} \text{ mm}^2/\text{s}$), and greater than the right temporoparietal ($1.230 \pm 0.114 \times 10^{-3} \text{ mm}^2/\text{s}$, $p < 0.001$) and left temporoparietal ($1.219 \pm 0.110 \times 10^{-3} \text{ mm}^2/\text{s}$, $p < 0.001$) regions.

FA values and their regional variations

The cortical grey matter FA values in the frontal region (0.138 ± 0.023) were similar to the left temporoparietal region (0.128 ± 0.030 , $p = 0.076$), and greater than the

Table 2. Regional variations in the reduced scattering coefficient, mean diffusivity and fractional anisotropy.

Head region	Mean	Standard deviation	<i>p</i> value (vs.)		
			Left temporo-parietal	Right temporo-parietal	Occipital
Reduced scattering coefficient (/cm)					
Frontal	5.98	1.23	0.006	<0.001	<0.001
Left temporo-parietal	6.59	1.22		<0.001	0.370
Right temporo-parietal	7.33	1.16			0.019
Occipital	6.95	1.40			
Average diffusivity ($\times 10^{-3}$ mm ² /s)					
Cortical grey matter					
Frontal	0.985	0.064	<0.001	<0.001	<0.001
Left temporo-parietal	0.919	0.041		0.465	0.021
Right temporo-parietal	0.929	0.052			1
Occipital	0.937	0.054			
Subcortical white matter					
Frontal	1.330	0.126	<0.001	<0.001	1
Left temporo-parietal	1.219	0.110		1	<0.001
Right temporo-parietal	1.230	0.114			<0.001
Occipital	1.319	0.165			
Fractional anisotropy					
Cortical grey matter					
Frontal	0.138	0.023	0.076	0.009	<0.001
Left temporo-parietal	0.128	0.030		1	0.004
Right temporo-parietal	0.126	0.030			0.033
Occipital	0.113	0.024			
Subcortical white matter					
Frontal	0.162	0.031	1	1	1
Left temporo-parietal	0.163	0.044		1	1
Right temporo-parietal	0.163	0.042			1
Occipital	0.156	0.045			

right temporoparietal (0.126 ± 0.030 , $p = 0.009$) and occipital (0.113 ± 0.024 , $p < 0.001$) regions (See Table 2 for other inter-region comparisons).

The subcortical white matter FA values were similar in the frontal (0.162 ± 0.031), left temporo-lateral (0.163 ± 0.044), right temporo-lateral (0.163 ± 0.042) and occipital (0.156 ± 0.045) regions.

Independent variables associated with the μ'_s value

Univariable analysis showed that greater μ'_s values were associated with greater gestational age at birth ($p = 0.035$), smaller FA values in the cortical grey matter ($p = 0.020$), smaller D_{av} values in the cortical grey matter and subcortical white matter ($p < 0.001$ and $p = 0.001$, respectively), smaller subarachnoid space ($p < 0.001$) and absence of brain abnormality ($p = 0.042$; Table 3 and Fig. 3). In the multivariable model, adjusted for the head region and gestational age at birth, greater μ'_s values were explained by smaller D_{av} in the subcortical white matter ($p < 0.001$), smaller subarachnoid space ($p < 0.001$) and

absence of brain abnormality ($p = 0.021$; Table 3). The findings from the alternative models, in which the D_{av} in the subcortical white matter was replaced with D_{av} in the cortical grey matter and FA in the cortical grey matter and subcortical white matter, are presented in Table 4. Greater μ'_s values were associated with smaller D_{av} values in the cortical grey matter ($p = 0.025$, Alternative model 1) and greater FA values in the subcortical white matter ($p = 0.005$, Alternative model 2), but not with FA in the cortical grey matter ($p = 0.476$, Alternative model 3) (Table 4).

Discussion

Using the qualitative and quantitative MRI information of the brain at term-equivalent age, we have demonstrated that the scattering property of near-infrared light was associated with macro- and microstructural information of the cerebral tissue in a cohort of preterm and term newborn infants. Specifically, greater light scattering was associated with smaller D_{av} values of the subcortical white matter and less severe brain abnormalities assessed

Table 3. Independent variables of the reduced scattering coefficient of near-infrared light.

Variables	Regression coefficient	95% confidence interval		<i>p</i>
		Lower	Upper	
Univariable analysis				
DTI measurement ¹				
D_{av} in cortical grey matter ($\times 10^{-3}$ mm ² /s)	-4.728	-7.063	-2.394	<0.001
D_{av} in subcortical white matter ($\times 10^{-3}$ mm ² /s)	-2.071	-3.311	-0.832	0.001
FA in cortical grey matter	-5.994	-11.032	-0.957	0.020
FA in subcortical white matter	3.806	-0.167	7.778	0.060
MRI assessment ¹				
Subarachnoid space (cm)	-0.289	-0.376	-0.201	<0.001
Brain abnormality	-0.422	-0.829	-0.015	0.042
Gestational age at birth ¹ (week)	0.065	0.005	0.125	0.035
Corrected age at TR-NIRS study ¹ (day)	0.004	-0.152	0.159	0.964
Head region				
Frontal	0	Reference		
Left temporo-parietal	0.617	0.295	0.940	<0.001
Right temporo-parietal	1.387	1.037	1.737	<0.001
Occipital	0.954	0.582	1.327	<0.001
Multivariable model ¹				
D_{av} in subcortical white matter ($\times 10^{-3}$ mm ² /s)	-2.066	-3.200	-0.932	<0.001
Brain abnormality	-0.400	-0.739	-0.061	0.021
Subarachnoid space (cm)	-0.314	-0.412	-0.216	<0.001
Gestational age at birth (week)	0.012	-0.038	0.061	0.648

D_{av} , average diffusivity; DTI, diffusion-tensor imaging; FA, fractional anisotropy; MRI, magnetic-resonance imaging; TR-NIRS, time-resolved near-infrared spectroscopy.

¹Adjusted for the four head regions.

on conventional MRI, even after adjusting for the subarachnoid space and other covariates. To the best of our knowledge, this is the first study to confirm the relationship between μ'_s and MRI findings obtained at term-equivalent age. With further validation studies, we believe that the μ'_s values might provide a clue to the mechanism of cerebral injury associated with preterm birth, subtle hypoxia-ischaemia, inflammation, poor nutrition and other covert but critical clinical events.

Light scattering and microstructural complexity of the brain

DTI measures of isotropic and anisotropic water diffusion have been used to assess the microstructural development of grey and white matter.^{28–30} Maturation in the grey matter was associated with a reduction in isotropic and anisotropic water diffusion, which is explained by the disruption of the highly radial organisation of the immature cortical plate by dendritic arborisation, synaptic formation, neuronal differentiation, intracortical white matter myelination and radial glia regression.^{28,29} Early stages of white matter maturation were associated with a reduction in isotropic and an increase in anisotropic water

diffusion, attributed to reduced water content, diminished extracellular spaces, increased complex microstructures, oligodendrocyte maturation and myelin formation.³⁰ In our current study, μ'_s showed consistent relationships with D_{av} and FA in the cortical grey matter and D_{av} in the adjacent white matter, suggesting that greater light scattering within the brain represents more mature cerebral tissue, confirmed by quantitative DTI measures.

Light scattering and the macrostructural feature of the brain

In addition to the water diffusion properties of the brain tissue, the μ'_s values of our study cohort were associated with an established qualitative score of brain abnormality for preterm infants, the relevance of which has extensively been demonstrated in relatively more mature infants.^{23,31} Considering that the items of this scoring system predominantly evaluate morphological features,^{3,23} the μ'_s values of the near-infrared light in the brain tissue might be determined by its micro and macrostructural features. Of the morphological information obtained from conventional MRI, we considered the subarachnoid space, located between the TR-NIRS probe and cerebral tissue,

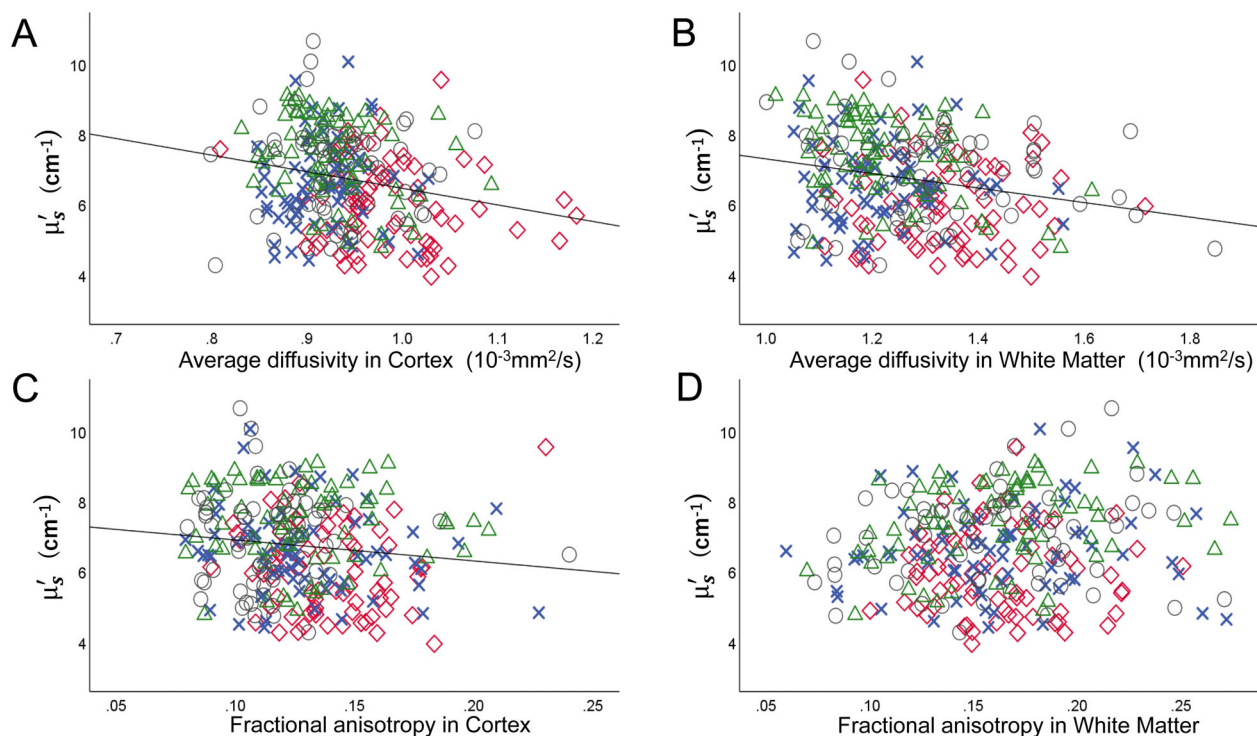


Figure 3. Relationships between diffusion-tensor biomarkers and reduced scattering coefficient of near-infrared light. Scatter plots showing associations between the reduced scattering coefficient (μ'_s) of near-infrared light and average diffusivity in the (A) cortical grey matter and (B) subcortical white matter and fractional anisotropy in the (C) cortical grey matter and (D) subcortical white matter. Regression lines are shown for convenience with p -values <0.05 from simple regression analysis without adjustment for covariates. Symbols: red open rhomboid, frontal region; blue cross, left temporo-parietal region; green open triangle, right temporo-parietal region; grey open circle, occipital head region.

Table 4. Alternative multivariable models to explain the reduced scattering coefficient of near-infrared light using different diffusion-tensor biomarkers.

Variables	Regression coefficient	95% confidence interval		p
		Lower	Upper	
Alternative model 1, incorporating grey matter average diffusivity				
D_{av} in cortical grey matter ($\times 10^{-3}$ mm ² /s)	-2.697	-5.054	-0.341	0.025
Brain abnormality	-0.416	-0.730	-0.102	0.009
Subarachnoid space (cm)	-0.309	-0.403	-0.215	<0.001
Gestational age at birth (week)	-0.002	-0.053	0.049	0.945
Alternative model 2, incorporating white matter fractional anisotropy				
FA in subcortical white matter	4.918	1.514	8.321	0.005
Brain abnormality	-0.390	-0.728	-0.052	0.024
Subarachnoid space (cm)	-0.319	-0.419	-0.219	<0.001
Gestational age at birth (week)	0.000	-0.052	0.051	0.988
Alternative model 3, incorporating grey matter fractional anisotropy				
FA in cortical grey matter	-1.810	-6.781	3.162	0.476
Brain abnormality	-0.315	-0.662	0.033	0.076
Subarachnoid space (cm)	-0.311	-0.408	-0.215	<0.001
Gestational age at birth (week)	0.004	-0.049	0.056	0.888

Models are also adjusted for the four head regions. D_{av} , average diffusivity; FA, fractional anisotropy.

as an important variable, potentially affecting the monitored μ'_s values. Further, μ'_s was negatively correlated with the subarachnoid space measurement, suggesting that a fraction of the near-infrared light passed through the subarachnoid space without being scattered. Although we do not have sufficient information to specify the fractions of light that passed through the subarachnoid space and cerebral tissue differently in our current study, relationships between μ'_s , D_{av} and MRI composite score were observed, even after adjusting for the measurement of the subarachnoid space. This confirms our hypothesis that μ'_s depended on the structural information of the cerebral tissue and extracerebral cerebrospinal fluid.

Aside from the potential influence of the subarachnoid space on light scattering, the tissue component spectrum through which the near-infrared light travels needs to be considered as well. The relationships between the quantitative DTI biomarkers and μ'_s observed in our current study were similar in the cortical grey and white matter. However, stating that μ'_s reflects the structural information of the superficial and deep brain structures would be a premature conclusion since the stage of tissue maturation, injury and remodelling would be similar in various tissue components in the same individual.^{32,33} Therefore, further studies are needed to delineate the precise dependence of μ'_s on various tissue components and the depth within the head.

Spatial differences in light scattering and water diffusion in the brain

Considerable spatial variations were observed in our study for the DTI biomarkers and μ'_s . Histological studies addressing the cortical grey matter development have highlighted the spatially heterogeneous caudal-to-rostral progression of cortex formation.³⁴ Recent neuroimaging studies have revealed that the timing of regional maturation is further regulated according to the local function, with the primary motor and sensory cortices differentiating before the cortical association areas.^{32,35} Furthermore, the white matter maturation follows a spatiotemporal pattern similar to that of the cortical grey matter, with posterior-to-anterior and central-to-peripheral directions.³⁶

Moreover, our study confirmed the spatially heterogeneous microstructures of the cortical grey and white matter, extrapolated from regional DTI biomarkers. The relatively high D_{av} and FA values of the frontal cortex suggested that this brain region matures slower than the other regions. The D_{av} values in the white matter of the frontal region were consistently the highest, while no spatial difference was noted for the FA values. The μ'_s values were the lowest in the frontal region and the highest in

the occipital region, which was consistent with the caudal-to-rostral progression of maturation.³⁴ Such agreements in the maturation-related spatial patterns of the measured variables between MRI, DTI and TR-NIRS provided further evidence supporting the hypothesis that the microstructural maturation process of the brain tissue could be non-invasively monitored using TR-NIRS.

Study limitations

First, our study cohort included both preterm and term hospitalised infants, who were likely to be different from their healthy peers in the developmental, maturational and healing processes of their brains. Second, as a significant relationship was observed between μ'_s and the subarachnoid space in our study, the μ'_s values obtained from the newborn head are likely to reflect the extracerebral information of the head, as well as anatomical information from the brain tissue. Third, considering that near-infrared light is efficiently absorbed by haemoglobin, μ'_s values might also be affected by blood haemoglobin levels. However, we have previously reported in a cohort of hospitalised preterm and term infants including the current study cohort that, although μ'_s and μ_a were tightly correlated between each other, only μ_a , but not μ'_s was correlated with blood haemoglobin levels, suggesting that the influence of haemoglobin to μ'_s values is small, if any.²¹ Finally, due to the limited schedule for the TR-NIRS data acquisition, we used MRI and TR-NIRS data obtained up to 6 days apart. However, the actual difference in the postnatal age between MRI and TR-NIRS studies was small (2.0 ± 2.5 days). Given that developmental changes in the MRI score, D_{av} and FA are noted over a few weeks basis,^{23,37,38} it is unlikely that the relationships between MRI and TR-NIRS variables observed in our current study were significantly obscured.

Conclusions

We demonstrated in a relatively large cohort of preterm and term newborn infants that the scattering property of near-infrared light was associated with the macro- and microstructural information of the cerebral tissue, as confirmed by conventional MRI-based scores and DTI biomarkers. However, the observed relationships between the light scattering property and MR markers of brain structures were not robust enough to provide a reliable estimation of MR abnormalities for specific newborn infants. Nonetheless, considering the non-invasive nature of TR-NIRS, data acquisition could be performed repeatedly at the cot-side in a large population of hospitalised infants, which may help accelerate the understanding of

covert clinical events responsible for subtle cerebral injuries and subsequent higher cognitive impairments.

Acknowledgements

The authors thank the infants who participated in the study and their families and the nursing staff at the Neonatal Intensive Care Unit, Kurume University Hospital. This study was funded by the Japanese Ministry of Education, Culture, Sports, Science and Technology (Grant-in-Aid for Scientific Research, 20H00102) and the Japan Science and Technology Agency (FOREST Program, JPMJFR2001).

Conflicts of Interest

The authors report no conflict of interest to declare.

Author Contributions

S. I., R. K., K. T., M. K., M. O., E. O., S. T., S. S. and O. I. contributed to conception and design of the study. S. I., R. K., K. T., M. K., YC. L., K. K., T. K., M. O., E. O. and O. I. contributed to the acquisition of data. S. I. and Y. A. analysed data. S. I. drafted the manuscript, which was critically reviewed and revised by R. K., K. T., M. K., YC. L., K. K., T. K., S. K., T. H., M. O., E. O., S. T., Y. A., S. S. and O. I. All authors approved the final version of the manuscript.

References

- Hack M, Flannery DJ, Schluchter M, Cartar L, Borawski E, Klein N. Outcomes in young adulthood for very-low-birth-weight infants. *N Engl J Med*. 2002;346(3):149-157.
- Iwata S, Nakamura T, Hizume E, et al. Qualitative brain MRI at term and cognitive outcomes at 9 years after very preterm birth. *Pediatrics*. 2012;129(5):e1138-e1147.
- Woodward LJ, Anderson PJ, Austin NC, Howard K, Inder TE. Neonatal MRI to predict neurodevelopmental outcomes in preterm infants. *N Engl J Med*. 2006;355(7):685-694.
- Dubois J, Dehaene-Lambertz G, Perrin M, et al. Asynchrony of the early maturation of white matter bundles in healthy infants: quantitative landmarks revealed noninvasively by diffusion tensor imaging. *Hum Brain Mapp*. 2008;29(1):14-27.
- Dubois J, Dehaene-Lambertz G, Kulikova S, Poupon C, Huppi PS, Hertz-Pannier L. The early development of brain white matter: a review of imaging studies in fetuses, newborns and infants. *Neuroscience*. 2014;276:48-71.
- Nossin-Manor R, Card D, Morris D, et al. Quantitative MRI in the very preterm brain: assessing tissue organization and myelination using magnetization transfer, diffusion tensor and T(1) imaging. *Neuroimage*. 2013;64:505-516.
- Panigrahy A, Nelson MD Jr, Bluml S. Magnetic resonance spectroscopy in pediatric neuroradiology: clinical and research applications. *Pediatr Radiol*. 2010;40(1):3-30.
- Thayyil S, Chandrasekaran M, Taylor A, et al. Cerebral magnetic resonance biomarkers in neonatal encephalopathy: a meta-analysis. *Pediatrics*. 2010;125(2):e382-e395.
- Wyatt JS. Cerebral oxygenation and haemodynamics in the foetus and newborn infant. *Philos Trans R Soc Lond B Biol Sci*. 1997;352(1354):697-700.
- Wolfberg AJ, du Plessis AJ. Near-infrared spectroscopy in the fetus and neonate. *Clin Perinatol*. 2006;33(3):707-728.
- Rolfe P. In vivo near-infrared spectroscopy. *Annu Rev Biomed Eng*. 2000;2:715-754.
- Sakudo A. Near-infrared spectroscopy for medical applications: current status and future perspectives. *Clin Chim Acta*. 2016;455:181-188.
- Patterson MS, Chance B, Wilson BC. Time resolved reflectance and transmittance for the non-invasive measurement of tissue optical properties. *Appl Optics*. 1989;28(12):2331-2336.
- Abrahamsson C, Lowgren A, Stromdahl B, et al. Scatter correction of transmission near-infrared spectra by photon migration data: quantitative analysis of solids. *Appl Spectrosc*. 2005;59(11):1381-1387.
- Beauvoit B, Liu H, Kang K, Kaplan PD, Miwa M, Chance B. Characterization of absorption and scattering properties for various yeast strains by time-resolved spectroscopy. *Cell Biophys*. 1993;23(1-3):91-109.
- D'Arceuil HE, Hotakainen MP, Liu C, Themelis G, de Crespigny AJ, Franceschini MA. Near-infrared frequency-domain optical spectroscopy and magnetic resonance imaging: a combined approach to studying cerebral maturation in neonatal rabbits. *J Biomed Opt*. 2005;10(1):11011.
- Zhang G, Katz A, Alfano RR, et al. Brain perfusion monitoring with frequency-domain and continuous-wave near-infrared spectroscopy: a cross-correlation study in newborn piglets. *Phys Med Biol*. 2000;45(11):3143-3158.
- Johnson LJ, Chung W, Hanley DF, Thakor NV. Optical scatter imaging detects mitochondrial swelling in living tissue slices. *Neuroimage*. 2002;17(3):1649-1657.
- Ijichi S, Kusaka T, Isobe K, et al. Developmental changes of optical properties in neonates determined by near-infrared time-resolved spectroscopy. *Pediatr Res*. 2005;58(3):568-573.
- Kurata T, Iwata S, Tsuda K, et al. Physiological and pathological clinical conditions and light scattering in brain. *Sci Rep*. 2016;6:31354.
- Iwata O, Iwata S, Kurata T, et al. Foetal growth, birth transition, enteral nutrition and brain light scattering. *Sci Rep*. 2021;11:21318.

22. Highton D, Tachtsidis I, Tucker A, Elwell C, Smith M. Near infrared light scattering changes following acute brain injury. *Adv Exp Med Biol.* 2016;876:139-144.
23. Kidokoro H, Neil JJ, Inder TE. New MR imaging assessment tool to define brain abnormalities in very preterm infants at term. *AJNR Am J Neuroradiol.* 2013;34(11):2208-2214.
24. Schneider CA, Rasband WS, Eliceiri KW. NIH image to ImageJ: 25 years of image analysis. *Nat Methods.* 2012;9(7):671-675.
25. Provenzale JM, Liang L, DeLong D, White LE. Diffusion tensor imaging assessment of brain white matter maturation during the first postnatal year. *Am J Roentgenol.* 2007;189(2):476-486.
26. Iwata S, Katayama R, Kinoshita M, et al. Region-specific growth restriction of brain following preterm birth. *Sci Rep.* 2016;6:33995.
27. Rubin M. When to adjust alpha during multiple testing: a consideration of disjunction, conjunction, and individual testing. *Synthese.* 2021;199:10969-11000.
28. Deipolyi AR, Mukherjee P, Gill K, et al. Comparing microstructural and macrostructural development of the cerebral cortex in premature newborns: diffusion tensor imaging versus cortical gyration. *Neuroimage.* 2005;27:579-586.
29. McKinstry RC, Mathur A, Miller JH, et al. Radial organization of developing preterm human cerebral cortex revealed by non-invasive water diffusion anisotropy MRI. *Cereb Cortex.* 2002;12:1237-1243.
30. Partridge SC, Mukherjee P, Henry RG, et al. Diffusion tensor imaging: serial quantitation of white matter tract maturity in premature newborns. *Neuroimage.* 2004;22(3):1302-1314.
31. Thompson DK, Warfield SK, Carlin JB, et al. Perinatal risk factors altering regional brain structure in the preterm infant. *Brain.* 2007;130(Pt 3):667-677.
32. Smyser TA, Smyser CD, Rogers CE, Gillespie SK, Inder TE, Neil JJ. Cortical gray and adjacent White matter demonstrate synchronous maturation in very preterm infants. *Cereb Cortex.* 2016;26(8):3370-3378.
33. Inder TE, Warfield SK, Wang H, Huppi PS, Volpe JJ. Abnormal cerebral structure is present at term in premature infants. *Pediatrics.* 2005;115(2):286-294.
34. Huttenlocher PR, Dabholkar AS. Regional differences in synaptogenesis in human cerebral cortex. *J Comp Neurol.* 1997;387(2):167-178.
35. Yu Q, Ouyang A, Chalak L, et al. Structural development of human fetal and preterm brain cortical plate based on population-averaged templates. *Cereb Cortex.* 2016;26(11):4381-4391.
36. Pecheva D, Kelly C, Kimpton J, et al. Recent advances in diffusion neuroimaging: applications in the developing preterm brain. *F1000Research.* 2018;7:F1000.
37. Bonifacio SL, Glass HC, Chau V, et al. Extreme premature birth is not associated with impaired development of brain microstructure. *J Pediatr.* 2010;157(5):726-32 e1.
38. Eaton-Rosen Z, Scherrer B, Melbourne A, Ourselin S, Neil JJ, Warfield SK. Investigating the maturation of microstructure and radial orientation in the preterm human cortex with diffusion MRI. *Neuroimage.* 2017;162:65-72.